Scale Dependence of Absorption of Photosynthetically Active Radiation in Terrestrial Ecosystems

Gregory P. Asner; Carol A. Wessman; Steve Archer

Ecological Applications, Vol. 8, No. 4 (Nov., 1998), 1003-1021.

Stable URL:
http://links.jstor.org/sici?sici=1051-0761%28199811%298%3A4%3C1003%3ASDOAOP%3E2.0.CO%3B2-X

Ecological Applications, 8(4), 1998, pp. 1003–1021

SCALE DEPENDENCE OF ABSORPTION OF PHOTOSYNTHETICALLY ACTIVE RADIATION IN TERRESTRIAL ECOSYSTEMS

GREGORY P. ASNER,[1,3] CAROL A. WESSMAN,[1] AND STEVE ARCHER[2]

[1]*Department of Environmental, Population, and Organismic Biology and Cooperative Institute for Research in Environmental Sciences, University of Colorado, Boulder, Colorado 80309-0216 USA*
[2]*Department of Rangeland Ecology and Management, Texas A&M University, College Station, Texas 77843 USA*

Abstract. The fraction of photosynthetically active radiation absorbed by plant canopies (fAPAR) is a critical biophysical variable for extrapolating ecophysiological measurements from the leaf to landscape scale. Quantification of fAPAR determinants at the landscape level is needed to improve the interpretation of remote sensing data, to facilitate its use in constraining ecosystem process models, and to improve synoptic-scale links between carbon and nutrient cycles. Most canopy radiation budget studies have focused on light attenuation in plant canopies, with little regard for the importance of the scale-dependent biophysical and structural factors (e.g., leaf and stem optical properties, leaf and stem area, and extent of vegetation structural types) that ultimately determine fAPAR at canopy and landscape scales. Most studies have also assumed that nonphotosynthetic vegetation (litter and stems) contributes little to fAPAR. Using a combined field measurement and radiative transfer modeling approach, we quantified (a) the relative role of the leaf-, canopy-, and landscape-level factors that determine fAPAR in terrestrial ecosystems and (b) the magnitude of PAR absorption by grass litter and woody plant stems.

Variability in full spectral-range (400–2500 nm) reflectance/transmittance and PAR (400–700 nm) absorption at the level of individual leaf, stem, and litter samples was quantified for a wide array of broadleaf arborescent and grass species along a 900-km north–south Texas savanna transect. Among woody growth forms, leaf reflectance and transmittance spectra were statistically comparable between populations, species within a genus, and functional types (deciduous vs. evergreen, legume vs. nonlegume). Within the grass life-form, spectral properties were statistically comparable between species and C_3/C_4 physiologies. We found that tissue-level PAR absorption among species, genera, functional groups, and growth forms and between climatologically diverse regions was statistically similar, and for fresh leaves, it represented the most spectrally similar region of the shortwave spectrum.

Subsequent modeling analyses indicated that the measured range of leaf, woody stem, and litter optical properties explained only a small proportion of the variance in tree and grass canopy fAPAR. However, the presence of nonphotosynthetic vegetation (e.g., stem and litter) had a significant effect on canopy fAPAR. In trees with a leaf area index (LAI) <3.0, stem surfaces increased canopy fAPAR by 10–40%. Standing grass litter canopies absorbed almost as much PAR as green grass canopies. Modeling the radiation regime in plant canopies should therefore account for the absorption of PAR by nonphotosynthetic plant components. Failure to do so may lead to overestimates of primary production, especially in woodlands, savannas, and shrublands dominated by species with optically thin canopies and in grasslands that accumulate senescent material.

Further sensitivity analyses revealed that the extent and LAI of vegetation structural types (trees and grasses) were the dominant controls on savanna landscape-level fAPAR, accounting for 60–80% of the total variation. Variation in leaf-level and all other canopy-level factors contributed individually to explain only a small proportion ($<11\%$) of the variance in landscape fAPAR; however, when considered as a group, they accounted for 20–40% of the variation in landscape fAPAR. These results emphasize the need for more mechanistic analyses of canopy-level radiative transfer, and subsequent carbon flux and trace gas processes, in plant canopies and across landscapes comprising heterogeneous mixtures of plant growth forms and life-forms.

Key words: canopy structure; leaf area index (LAI); leaf optical properties; litter; photosynthetically active radiation (PAR) absorption; principal components analysis; Prosopis glandulosa; *radiative transfer; remote sensing; savannas; scaling; scattering.*

Manuscript received 27 August 1997; accepted 9 February 1998.
[3]Address for reprints: CIRES/CSES, Campus Box 216, University of Colorado, Boulder, Colorado 80309-0216 USA.

Introduction

The chemical composition and radiative characteristics of the atmosphere are significantly affected by the extent and biophysical attributes of terrestrial vegetation (e.g., Ciais et al. 1995, Denning et al. 1995, Sellers et al. 1997). Shortwave energy (400–3000 nm) from the sun may be absorbed by plant tissue and soils, re-emitted as longwave energy (e.g., heat), or reflected back into space, contributing to the earth's albedo. The presence of chlorophyll, carotenes, and other pigments in leaves enables plant canopies to strongly absorb photons in the photosynthetically active radiation (PAR) region of the spectrum (400–700 nm) (Salisbury and Ross 1969, Wooley 1971, Maas and Dunlap 1989). The fraction of PAR absorbed by plant canopies (fAPAR) significantly affects canopy photosynthesis, carbon assimilation and evapotranspiration rates (e.g., Ehleringer and Pearcy 1983, Baldocchi and Hutchinson 1986, Collatz et al. 1991, Norman 1993). To date, the determinants of PAR absorption variability in canopies and across landscapes have not been well quantified despite implications for scaling processes of CO_2 exchange, water flux, trace gas emissions, and net primary production (NPP) to landscape, regional, or global levels.

Synoptic-scale fAPAR estimates are needed as input to many biogeochemical, biosphere–atmosphere, and climate models (e.g., Field et al. 1995, Sellers et al. 1997). Satellite-based methods are currently the only feasible way of acquiring fAPAR estimates at the temporal and spatial scales necessary for these modeling approaches (Sellers 1987, Schimel 1995, Asner et al. 1998*a*, Wessman and Asner 1998). However, remotely sensed pixels typically contain mixtures of vegetative materials (leaves, stems, litter) and vegetation types (trees, shrubs, grasses). An understanding of the relative importance of these factors and the way they interact to influence variation in fAPAR across landscapes and within biomes is therefore needed (Asrar et al. 1992, Asner and Wessman 1997).

Assessment of fAPAR in ecosystems is scale dependent. The radiation regime of plant canopies is the integrated outcome of photon scattering by leaves, stems, and soils. Soil reflectance characteristics are a function of moisture content, surface texture, and parent material (Stoner and Baumgardner 1981, Jacquemoud et al. 1992). Leaf-level scattering characteristics (or leaf optical properties) are primarily determined by leaf structure and chemistry, including water content, the concentration of structural carbon constituents (e.g., cellulose, lignin), chlorophyll, and other biologically active pigments (Gates et al. 1965, Thomas et al. 1971, Wooley 1971, Walter-Shea and Norman 1991, Fourty et al. 1996). Scattering by stem surfaces is influenced by carbon constituents, roughness, and moisture (Murray and Williams 1987, Asner and Wessman 1997). At the canopy scale, the contribution of leaf, stem, and soil optical properties to fAPAR is modulated by leaf area index (LAI), leaf angle distribution (LAD), and foliage clumping, which determine the density and optical depth of a plant canopy (Ross 1981). As a result, total canopy radiation absorption cannot be predicted solely from a knowledge of the absorption and scattering properties of leaves, stems, and soils (Myneni et al. 1989, Norman 1993). Similarly, the organization of individual canopies or vegetation patches influences the radiation regime at the landscape level, but other factors, such as shadowing between canopies and patches, become an important consideration (Li and Strahler 1985, Asner and Wessman 1997). The extent to which properties characterizing and processes operating at lower levels of ecological organization (e.g., leaf and stem optics) are important in explaining or predicting properties and processes emerging to control fAPAR at higher levels of ecological organization (e.g., landscapes) are not yet clear.

Canopy-level estimates of PAR absorption or interception have often been acquired through measurements of downwelling and/or upwelling energy along vertical profiles. In dense, horizontally homogeneous canopies, these light attenuation methods can adequately represent the PAR regime for canopy photosynthesis and carbon assimilation studies (Norman 1979, Baldocchi 1992, 1993). However, the results of light attenuation studies, and statistical models derived from attenuation studies, can be difficult to apply to new environments (Nilson 1971, Norman 1993). Moreover, nonphotosynthetic materials including twigs, branches, stems, senescent foliage, and soils absorb PAR (van Leeuwen and Huete 1996, Asner and Wessman 1997); canopy radiation budget studies generally assume little to no contribution from nonphotosynthetic vegetation in determining fAPAR.

Advances in radiative transfer modeling now provide a means to assess the canopy radiation regime from a physical and mechanistic basis. The newest models are based on the physics of photon scattering, and range in complexity from one-dimensional (vertical profile) algorithms to sophisticated three-dimensional landscape simulations (e.g., Shultis and Myneni 1988, Liang and Strahler 1993, Myneni and Asrar 1993, Kuusk 1995, Asner and Wessman 1997). Since some of these models can simulate the scattering characteristics of leaves, stems, and soils, they can be used to explore the shortwave radiation regime within plant canopies and across landscapes. In this study, we used a combination of field and modeling methods to quantify the relative importance of the leaf, canopy, and landscape biophysical and structural characteristics that drive fAPAR variability in terrestrial ecosystems. Our focus begins at the level of individual leaf, woody stem, and standing litter optical properties (biophysical attributes of plants), then extends to the structure of whole canopies and upward to a heterogeneous savanna land-

scape comprising contrasting vegetation types (trees vs. grasses). Our intention was to uncover which factors most strongly drive changes in the PAR regime at the scale of whole ecosystems or regions. In remote sensing terms, we were interested in the relative importance of plant (species-specific leaf, stem, and litter optics), canopy (LAI and plant architecture), and patch (diverse mixtures of trees and grasses) properties and how these might interact to determine fAPAR within a satellite image pixel.

Our specific objectives were threefold. We first quantified the reflectance and transmittance properties of leaves, woody stems, and standing litter in both the PAR (400–700 nm) and entire shortwave (400–2500 nm) spectral ranges. We were particularly interested in documenting the extant differences within and among species, genera, growth forms, life-forms and functional groups along a climatic gradient. We then determined the relative importance of the measured tissue optical property variation on canopy fAPAR using a physically based radiative transfer model. Finally, we quantitatively assessed the relative importance of leaf, stem, and litter optical properties, canopy structure, and landscape-level organization of canopies in determining PAR absorption at the ecosystem level.

PAR Absorption vs. Interception by Plant Canopies

Many previous canopy PAR studies have confused the subtle but important differences between the fraction of PAR *absorbed* (fAPAR) and *intercepted* (fIPAR) by plants, and for this paper, it is essential that the distinction be made. fIPAR is the fraction of incoming PAR captured by plant tissues as it scatters down through the canopy:

$$\text{fIPAR} = \frac{\text{PAR}_i - \text{PAR}_t}{\text{PAR}_i} \quad (1)$$

where PAR_i is the incident PAR at the top of the canopy, and PAR_t is the amount of PAR exiting the bottom of the canopy. fIPAR accounts for neither the PAR that scatters from the canopy back into the atmosphere nor the PAR that scatters from the soil or litter surface back into the canopy where it is absorbed or lost to the atmosphere.

fAPAR is the fraction of incoming PAR absorbed by a plant canopy, accounting for scattering losses (PAR_s) from the canopy to the atmosphere ($\text{PAR}_{s(\text{canopy})}$), and the photons scattered by the soil or litter surface into atmosphere without being absorbed by the plant canopy ($\text{PAR}_{s(\text{bottom})}$):

$$\text{fAPAR} = \frac{(\text{PAR}_i - \text{PAR}_t - \text{PAR}_s)}{\text{PAR}_i} \quad (2)$$

where

$$\text{PAR}_s = \text{PAR}_{s(\text{canopy})} + \text{PAR}_{s(\text{bottom})}.$$

In canopies comprising dense green leaf material (e.g., some croplands), the scattering term (PAR_s) may be small (3–10%) and subsequently ignored (Russell et al. 1989), making fIPAR a reasonable estimate of fAPAR. However, in areas with open canopies or in which nonphotosynthetically active tissue (stems, standing litter) may be present, fIPAR and fAPAR can be quite different (Prince 1991). Although fIPAR requires fewer flux measurements than fAPAR (e.g., Goward and Huemmrich 1992, Walter-Shea et al. 1992), most studies attempting to scale leaf-level processes (e.g., gas exchange) to canopy and landscape scales require fAPAR, as this is the quantity that permits the most robust functional link between scales (Sellers 1987, Wessman and Asner 1998). For this reason, we focus on the scale dependence of fAPAR in canopies and across landscapes. We use fIPAR measurements, which are obtained more expediently than fAPAR measurements, only to assess performance of the radiative transfer model.

Methods

Study sites

Savannas and shrublands cover ~25% of the global terrestrial surface (Matthews 1983). These regions endure some of the highest anthropogenic land-use pressures on earth, including intensive grazing and altered fire regimes (Tothill and Mott 1985, Crutzen and Andreae 1990, Young and Solbrig 1993, Archer 1994), leading to sharp variation in the relative proportion of vegetation cover types (e.g., woody and herbaceous plants). Under both natural and managed conditions, savannas are spatially and temporally complex, with significant heterogeneity occurring at meter scales (e.g., Florian et al. 1996). The savanna physiognomy, with arborescent canopies imbedded in a complex matrix of live and senescent herbaceous species (usually grasses), provides an excellent prototype environment for exploring the factors influencing fAPAR in structurally complex ecosystems.

Three primary savanna types occur along a 900-km north–south transect extending from Vernon to Alice (La Copita), Texas (Fig. 1, Table 1): (1) *Prosopis glandulosa* savanna grasslands near Vernon, (2) *Quercus/Juniperus* savanna parklands near Sonora, and (3) *Acacia/Prosopis* savanna parklands at La Copita. While all of these savannas comprise a spatially heterogeneous mixture of woody and herbaceous species, each contains a unique combination of globally common savanna, shrubland, woodland, and grassland genera. The northernmost site, located on the 200 000 ha Waggoner Ranch near Vernon, Texas, was characterized by the microphyllous leguminous tree *Prosopis glandulosa* var. *glandulosa* (honey mesquite), an herbaceous layer dominated by C_3 and C_4 grasses, and occasional riparian zones containing a variety of broadleaf arborescent species. The central site was located at the Texas A&M Sonora Research and Extension Center on the south-

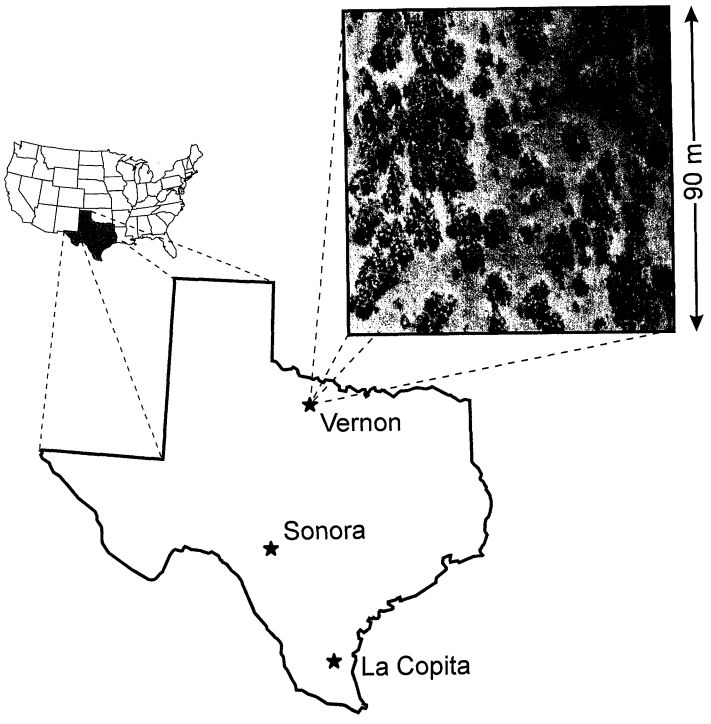

FIG. 1. The 900-km north–south Texas savanna transect used for the leaf, stem, and litter optical properties survey. An extensive analysis of canopy structure at the North Texas (Vernon) savanna site was completed in an effort to evaluate radiative transfer model performance. The aerial photograph of a typical 90 × 90 m area at the northern site shows the scattered *Prosopis* trees of varying size and spacing embedded in a matrix of C_4 grasses. Shadowing within and between canopies is apparent.

west edge of the Edwards Plateau. The vegetation was dominated by two oak (*Quercus*) and two *Juniperus* species with many secondary woody and C_4 grass species. The southernmost site was located near Alice, Texas, at the Texas A&M La Copita Research Area. The La Copita site was composed of C_4 grasses and a diverse assemblage of woody growth forms, dominated by *P. glandulosa* and several *Acacia* species. Differences in mean annual precipitation and temperature, length of growing season, and percent woody cover along this transect are summarized in Table 1.

Leaf, woody stem, and standing litter optical properties were determined for numerous tree, shrub, and grass species at each site. The North Texas (Vernon) site was used for the canopy radiative transfer model evaluation and analysis because it contained the simplest landscape structural layout while still providing sharp vegetation cover contrasts (Fig. 1). A localized east (550 mm/yr)–west (665 mm/yr) precipitation gradient across a 40 km distance, coupled with ongoing grazing and prescribed fire experiments at the North Texas site, provided a range of aboveground biomass levels required for model evaluation exercises, while still maintaining similar species composition.

Tissue optical properties

Leaves of arborescent species (trees and shrubs) at each site were sampled by clipping 5–10 branches from individual plants, which were sealed in airtight polyethylene bags and stored in a cooler until the spectra were measured. Green grass and standing litter samples were collected by placing whole grass clumps (including some roots and soil) into bags to maintain leaf moisture. Spectral measurements were conducted within 15 min of sample collection. Hemispherical reflectance and transmittance values (400–2500 nm) were

TABLE 1. Tree, shrub, and grass foliage, stem, and standing litter samples were collected along a latitudinal gradient extending from northern to southern Texas, USA.

Site name	Resource area[1]	Location (latitude)	MAT (°C)	Annual PPT (mm)	Growing season (d)	Woody cover (%)	Dominant vegetation
Vernon[2]	Rolling Plains	33°57′ N	17	620	220	20–50	*Prosopis glandulosa*, savanna grassland
Sonora[3]	Edwards Plateau	30°10′ N	20	575	240	10–30	*Quercus-Juniperus*, savanna parkland
La Copita[4]	Rio Grande Plains	27°40′ N	22	680	290	30–70	*Prosopis-Acacia*, savanna parkland

Notes: MAT = mean annual temperature; PPT = precipitation. For detailed summaries of climate, soils, and vegetation see [1] McMahon et al. (1984), [2] Heitschmidt et al. (1986), [3] Amos and Gehlbach (1988), [4] Archer (1995).

obtained using a full-range spectroradiometer (Analytical Spectral Devices, Inc., Boulder, Colorado), a $BaSO_4$ integrating sphere (LI-1800, LI-COR Inc., Lincoln, Nebraska), and a light source modified for full-range spectral measurements. The ASD spectrometer acquired measurements at 1.4-nm intervals in the visible/near-infrared (NIR) and at 2.0-nm increments in the shortwave infrared (IR) (SWIR) region. Each reflectance and transmittance spectrum represented the mean of 200 individual spectral measurements.

A modified version of the Daugherty et al. (1989) method for spectral analyses of needle leaves was used for the leaflets of species not completely covering the sample port on the integrating sphere (e.g., *Acacia, Prosopis,* green and senescent grass leaves). Procedural errors can produce negative transmittance values when the gap fraction between leaves placed over the sample port is large. We used techniques developed by Middleton et al. (1996) and M. A. Mesarch et al. (*unpublished data*) to decrease the gap fraction in the sample port to <20%, thus minimizing this problem.

Woody stem material was collected from trees and shrubs by removing thin, opaque slices of the outer bark. Flat areas on the stems were selected to ensure that the sample port of the integrating sphere would close properly. Reflectance spectra were collected from 5 to 10 individuals of each species, with each sample consisting of a 200-spectrum average.

A general analysis of the variability in tissue optical properties across the 400–2500 nm spectral range was first conducted to uncover potential differences among species, genera, functional groups, life-forms and growth forms. A total of 350 arborescent and grass leaf, 245 woody stem, and 105 standing litter samples from 38 different tree, shrub, and grass species were compared. Leaves varied significantly in morphology, roughness, pubescence, and thickness. The mean and standard deviation of the reflectance and transmittance values of species, genera, and functional groups were compared with the overall arborescent and grass life-form mean values (Student *t* tests). *Prosopis glandulosa* occurred at all three sites, so we were able to quantify intraspecies variation in leaf and stem spectra along the Texas transect. Comparisons within species (=population variation) and among species within genera were also made using three *Quercus* (two from Sonora, one from Vernon) and four *Acacia* species (all from La Copita).

Leaf, woody stem, and litter fractional PAR absorption values ($fAPAR_{tissues}$) were then calculated for each species:

$$fAPAR_{tissues} = \frac{\sum_{\lambda=400}^{700} (1.0 - \rho_\lambda - \tau_\lambda)}{301} \quad (3)$$

where ρ_λ is the hemispherical reflectance at wavelength λ and τ_λ is the hemispherical transmittance. $fAPAR_{tissues}$ was then compared among species, genera, functional groups, and growth forms. Variability in tissue-level fAPAR within these groups was compared with that of the entire aborescent and grass life-form groups (Student *t* tests).

Measurements of canopy structure and fIPAR

Canopy structure and intercepted PAR variability were quantified at the North Texas *Prosopis* savanna site. These data were then used to evaluate the performance of the radiative transfer model and to parameterize it for later sensitivity analyses. Ten 60 × 60 m plots were established by randomly placing 1–2 plots in rangelands with different livestock grazing and prescribed burning regimes across the local east–west precipitation gradient. In July 1996, grass canopy fIPAR and LAI were measured at 5-m intervals along two transects extending diagonally across each plot (n = 36 sample points per plot). Each fIPAR point consisted of an average of four measurements using a line quantum sensor (LI-191SA, LI-COR Inc., Lincoln, Nebraska) oriented along (one measurement forward and one backward of sampling point) and perpendicular to the transect (left and right of the sampling point). Incoming radiation was monitored with a stationary point quantum sensor (LI-190SA, LI-COR Inc., Lincoln, Nebraska) mounted on a tripod situated to obtain a clear view of the sky. Dataloggers on the roving line and stationary point quantum sensors were synchronized for later fIPAR calculations. fIPAR measurements were acquired on clear sky days within one hour of solar noon. The fraction of PAR intercepted (fIPAR) by the grass canopy was estimated using

$$fIPAR = \frac{1}{PAR_i}\left(PAR_i - \frac{\sum_{p=1}^{4} PAR_t}{4}\right) \quad (4)$$

where PAR_i is the total incoming radiation in the 400–700 nm range, and PAR_t is the energy transmitted through the canopy, summed, and averaged for the four measurements at each sample point.

When *Prosopis* trees were encountered, PAR transmitted through the canopy was measured above the grass understory at two locations along the long axis of the crown and two locations perpendicular to the long axis (n = 4 per crown). The fIPAR of each tree canopy was calculated using Eq. 4. When <15 *Prosopis* trees were encountered along transects within a plot, additional individuals were randomly chosen until a minimum of 15 trees were characterized.

Prosopis plant area index (PAI = LAI + Stem AI) and grass PAI (=LAI + Litter AI) were estimated at each fIPAR sampling point using a plant canopy analyzer (LAI-2000, LI-COR Inc., Lincoln, Nebraska). Measurements were acquired on fully overcast days, as the calculations made by the instrument's computer assume diffuse (isotropic) sky conditions. A three-quarter view cap was used to prevent errors from the

user's silhouette or from viewing too much clear sky (LI-COR 1992). PAI values were based on the mean of four readings (as per fIPAR measurements).

The plant canopy analyzer should be calibrated against actual measurements when used on species with discrete crowns such as the *Prosopis* trees in this study. We calibrated the canopy analyzer readings by destructively harvesting trees representing the range of canopy architectures and sizes common to the study plots and measuring LAI with a leaf area meter (J. Ansley and G. P. Asner, *unpublished data*). This comparison yielded the relationship for *Prosopis* trees:

$$LAI_{Actual} = 1.76(PAI_{LI\text{-}COR}) + 0.13 \quad (5)$$

($r^2 = 0.84$, $n = 10$). Stem area index (SAI) of *Prosopis* was also estimated by obtaining plant canopy analyzer readings before and immediately after *Prosopis* defoliation. Measurements were collected in the same manner as for the intact crowns, and a relationship similar to that of Eq. 5 was used to correct the data.

At each grass sampling point along the transects, a 1 m^2 area was marked, and the relative cover of live grass and standing litter was visually estimated in 10% increments. Three observers recorded their estimates independently, and these were then averaged.

Leaf inclination, an important factor for canopy radiative transfer modeling (Ross 1981, Campbell 1986), was estimated on three *Prosopis* trees in each plot. Because *Prosopis* has compound leaves, we characterized the angle of the leaflets. One hundred leaflets were randomly selected on each tree, and a leaf inclinometer was used to estimate the angle from horizontal. The inclination angle of *Prosopis* stems and branches was also measured (n = 10–20 per individual). Estimates of the inclination angle of live and standing litter herbaceous biomass in each of the 60 × 60 m main plots were based on 60 measurements in each of three 1-m^2 plots randomly selected from among the 36 sample points encountered along transects. Distribution functions describing the leaf orientation of *Prosopis* trees and the grass understory were derived from these data.

Crown height and width were measured on the same *Prosopis* trees used for the leaf angle measurements (n = 30 for all plots combined). These crown dimensions were used to parameterize the overstory *Prosopis* canopy in the landscape radiative transfer model. The areal extent of tree, herbaceous, and bare soil cover was estimated in each plot using a combination of low-altitude color-IR aerial photographs and field observations. Air photos acquired in June 1994 were scanned into digital format, and the three primary covertypes were calculated using an image processing software package (ENVI, Research Systems, Inc., Boulder, Colorado).

Canopy radiative transfer modeling

We used a three-dimensional landscape radiative transfer model (discrete ordinates solution) capable of handling two or more vegetation types, each with varying canopy structure, self-shadowing, and shadowing between canopies. Based on the model originally developed by Myneni and Asrar (1993), details on its formulation and additional components are given by Li and Strahler (1985), Marshak (1989), Myneni and Asrar (1993), and Qin (1993). While computationally expensive, three-dimensional models are currently the only reliable method for quantitatively assessing the radiation regime in spatially complex, multi-element canopies (Asrar et al. 1992). Briefly, the main components of the model are as follows:

(i) The model is based on modified turbid medium theory, which approximates a canopy as a volume of leaf and stem elements with canopy gaps. Photons interact with canopy elements through both single and multiple collisions, and photons are permitted to travel in 96 directions, 12 directions per octant of a unit sphere (Myneni and Asrar 1993).

(ii) Scattering of photons by individual leaves and stems sections is parameterized using measured hemispherical reflectance and transmittance values (Asner and Wessman 1997). The specular component of leaf reflectance is also simulated (Marshak 1989). Scattering at the soil surface is isotropic and is parameterized using field measurements of soil reflectance.

(iii) Canopy structure is simulated using leaf and stem area indices, leaf and stem zenith angle distributions, and an index of foliage clumping. Photons are scattered and absorbed in three-dimensional space, and interactions with the soil surface (reflection and absorption) and the atmosphere (scattering losses) are simulated. Leaf and stem azimuthal angles are modeled as a uniform distribution.

(iv) Shadowing between canopies and vegetation types is simulated using a geometric-optical model in which tree crowns are approximated as ellipsoids (Li and Strahler 1985). Crown dimensions are parameterized using field allometric measurements.

(v) Both canopy- and landscape-level radiation regimes are dependent on sun position and sky conditions (Ross 1981). The model simulates the physical interaction of both direct beam and diffuse radiation with the canopy. For this comparative study, we placed the sun at 12° zenith and 165° azimuth to simulate northern Texas savanna illumination at solar noon on 15 July 1996. Sky conditions were simulated as relatively clear (80% direct/20% diffuse incoming radiation).

The model can also be used in one-dimensional mode, thus simulating the photon transport in a single vegetation type. We employed the one-dimensional mode when considering the effects of leaves, stems, litter, and soils on single-canopy fAPAR.

It is important to emphasize that the model simulates the interaction of photons within canopies based on the scattering characteristics derived for plant tissue and soil surfaces. It does not calculate canopy absorption

directly from leaf or stem absorption. Instead, the model allows for photons to scatter throughout a canopy, and then calculates fAPAR after all scattering events have occurred.

Canopy model evaluation

In addition to modeling canopy fAPAR, the total photon flux exiting the bottom of the canopy can be calculated to simulate fIPAR. To evaluate the accuracy of the radiative transfer model in simulating canopy PAR, we compared modeled and measured fIPAR for tree and grass covers at the northern Texas (Vernon) site. Leaf, woody stem, standing litter, and soil spectral data and the measured canopy structural characteristics were used to simulate fIPAR for half of the herbaceous and all of the tree sample points in each of the ten 60 $\times$ 60 m plots (n = 180 for grass plots, n = 150 for trees). *Prosopis* canopies and grass plots were simulated separately to evaluate the model's accuracy in predicting canopy fIPAR for these vegetation types.

Canopy and landscape sensitivity analyses

Following the fIPAR modeling evaluation, our focus turned to the determinants of fAPAR in individual plant canopies. A series of sensitivity analyses was performed to quantify the importance of the measured variability of leaf, woody stem, and litter optical properties in determining fAPAR at the canopy level. Separate simulations of arborescent and grass canopies utilized the mean and variance of leaf, woody stem, and litter optical properties obtained from tree, shrub, and grass species along the north–south Texas savanna transect. These analyses allowed us to quantify the individual contribution of leaves, stems, and litter to the PAR regime under different LAI scenarios for each vegetation type (woody and graminoid).

Landscape-level determinants of PAR absorption variability were assessed by combining the field and modeling components into one perturbation analysis. Using the total observed variability in leaf optical and canopy and landscape structural characteristics, 250 base-case savanna landscape simulations were performed. Values for leaf-, canopy-, and landscape-level parameters (tissue optical properties; leaf and stem area indices; relative extent of tree and grass covers) were randomly selected within their observed range, and a landscape fAPAR value was generated. For every base-case simulation, each parameter was, in turn, perturbed by $\pm$10% of its ecologically realistic range, and the simulation repeated for each scenario. We chose $\pm$10% based on the assumption that smaller changes would generally be undetectable using current field methods. For example, a change in LAI from 1.0 to 1.1 is probably not significant, since the error in measuring LAI in the field is typically of equal or greater order.

A database was created for all model simulations (n = 250 base case + 250 $\times$ 10 perturbed parameters = 2750 model runs). The sum of squares of differences, or merit-of-change value, between the original landscape fAPAR value and the value derived following each parameter perturbation was recorded. This statistic indicated the sensitivity of landscape fAPAR to a $\pm$10% change in a parameter. The results were binned according to sum of the landscape component LAIs (tree + grass), and within each bin, a principal components analysis was performed on the merit-of-change values. Since the first principal component axis represents the direction of maximum variance, the weighting of each perturbed parameter's contribution to that axis was a measure of the model's sensitivity to the perturbation (Privette et al. 1994, Asner, 1998). This allowed us to derive a sensitivity index for all perturbed parameters within each LAI bin. Thus, the index provided a means to test the contribution of each scale-dependent biophysical and structural variable to the landscape fAPAR regime.

RESULTS

Leaf optical properties

Mean ($\pm$1 SD) hemispherical reflectance and transmittance properties of fresh grass and woody plant leaves are shown in Fig. 2. Among woody growth forms, neither leaf reflectance nor transmittance spectra differed significantly among genera, growth forms, or functional types (e.g., deciduous vs. evergreen, legume vs. nonlegume; $P > 0.05$, t tests at each wavelength), thus they were pooled together as a single group. There were many species-specific differences at various wavelengths, but these differences were inconsistent even among samples within a single species. The variability within genera, growth form, and functional groups always exceeded that of any single species, but no single species was significantly different from these groupings (t tests by wavelength). Within the grass lifeform, we also found no statistical differences between genera or C_3/C_4 physiology. Again, the variance within any given species tended to be less than that observed by genus or photosynthetic pathway, but no general trends or differences could be found.

A comparison of woody plant vs. graminoid lifeforms revealed consistently higher leaf reflectance values for grasses throughout the visible region (t tests at each wavelength, $P < 0.05$), whereas woody species had higher values throughout the NIR region (t tests, $P < 0.05$; Fig. 2A). There were no significant reflectance differences between woody plant and grass leaves in the shortwave IR (SWIR) range. Among woody plants, leaf reflectance variability was lowest in the PAR region (CV = 6–8%), and highest in the SWIR near 2400 nm (CV = 21–23%). Among grasses, the lowest leaf reflectance variation was in the PAR region (CV = 6–7%), while the highest was in the NIR (CV = 10–11%). Conservative scattering in the visible range results from the biochemical constraints imposed by the presence of chlorophyll (Gausman 1982, Boyer

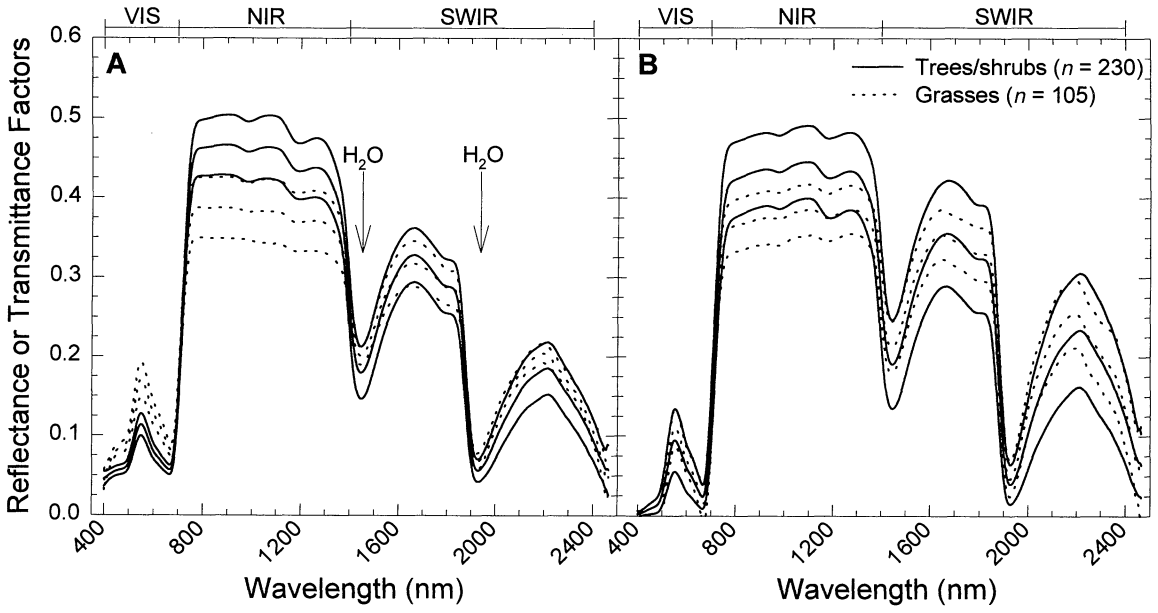

FIG. 2. Shortwave (400–2450 nm) hemispherical reflectance (A) and transmittance (B) values for broadleaf arborescent and grass species collected along the north–south Texas savanna transect. Solid lines depict mean (±1 SD) of arborescent species, and dotted lines represent mean (±1 SD) of grass species. Visible (VIS), near-infrared (NIR), and shortwave-infrared (SWIR) spectral regions are indicated. Strong water absorption features near 1400 and 1900 nm are also delineated.

et al. 1988, Maas and Dunlap 1989, Walter-Shea and Norman 1991, Poorter et al. 1995). A comparison of the woody plant and grass leaf transmittance spectra showed no statistically significant differences throughout the entire shortwave region (Fig. 2B).

Strong absorption features near 450 and 680 nm are associated with chlorophyll and other pigments (Salisbury and Ross 1969, Danks et al. 1984), while the strong increase in reflectance and transmittance in the near-infrared (NIR) is due to scattering of photons at the air–cell interfaces within the spongy mesophyll (Wooley 1971, Boyer et al. 1988, Walter-Shea et al. 1992). The two "dips" along the NIR plateau (1000 and 1200 nm) were most pronounced in woody plants and are weak water absorption features (Gao and Goetz 1995). In the SWIR range (1200–2450 nm), the spectra are dominated by water absorption, which obscures leaf biochemical features related to the concentration of lignin and other carbon constituents (Curcio and Petty 1951, Wooley 1971, Fourty et al. 1996). Thus, the general increase in reflectance and transmittance variability in the NIR and SWIR regions is primarily driven by leaf-level differences in water content (Gao and Goetz 1995). While it is well known that water content dominates the NIR/SWIR leaf reflectance and transmittance properties, quantification of the relative importance of water, carbon, and nitrogen continues to be difficult (Curran et al. 1992, Fourty et al. 1996).

Upon convolving the leaf reflectance and transmittance spectra in the PAR (400–700 nm) range, we found no significant differences between like species or genera from different geographic locations, nor between genera or functional types (Table 2). There were some species-specific differences (e.g., *Prosopis* vs. *Q. virginiana,* $P < 0.05$), but these occurrences were few and no consistent pattern was evident. Among woody species, leaf absorptance values ranged from 83 to 93%, with a mean ± 1 SD of 90 ± 2%). The variance in leaf PAR absorption was comparable (CV = 2–3%) across all groups of species, genera, growth forms, and sites. Leaf-level PAR absorption was also quite similar among grass species, with a mean of 87 ± 2% (Table 3). While slightly lower than the mean for woody species (Table 2), the difference between woody plant and grass groups was not statistically significant ($P = 0.12$, t test).

The mass, thickness, and chlorophyll concentration of leaves can dynamically interact to maintain relatively similar leaf optical properties in the PAR region, even along strong gradients of light intensity within canopies (e.g., Lee and Graham 1986, Poorter et al. 1995). Our results further suggest that leaf absorptance among grasses and broadleaf woody plant growth forms is dynamically stable along a pronounced climatic gradient. We did not explicitly assess leaf-level PAR absorption for a wide range of leaf ages, although some of this variability was naturally present in our samples. While age can affect leaf optical properties, the effects in the PAR region are typically small until senescence occurs (e.g., Horler et al. 1983, Boyer et al. 1988). We thus chose to focus on the fully expanded leaves since they comprise the bulk photosynthetic vol-

TABLE 2. Variability of woody plant leaf and stem optical properties in the PAR spectral range.

Species	Fresh leaf material			Stem material	
	Absorptance	Reflectance	Transmittance	Absorptance	Reflectance
Prosopis glandulosa (1) (L)	0.85 (0.03)	0.07 (0.01)	0.08 (0.03)	0.91 (0.03)	0.09 (0.03)
Prosopis glandulosa (2) (L)	0.87 (0.01)	0.07 (0.00)	0.05 (0.01)	0.92 (0.01)	0.08 (0.01)
Prosopis glandulosa (3) (L)	0.89 (0.01)	0.07 (0.00)	0.04 (0.00)	0.92 (0.05)	0.08 (0.05)
All *Prosopis*	0.87[a] (0.02)	0.07[b] (0.00)	0.06[c] (0.02)	0.92[d] (0.04)	0.08[e] (0.04)
Acacia berlandieri (3) (L)‡	0.92 (0.01)	0.06 (0.00)	0.02 (0.01)	0.93 (0.01)	0.07 (0.01)
Acacia farnesiana (3) (L)‡	0.86 (0.02)	0.08 (0.00)	0.06 (0.02)	0.90 (0.01)	0.10 (0.01)
Acacia greggii (3) (L)‡	0.91 (0.01)	0.08 (0.00)	0.02 (0.01)	0.87 (0.02)	0.13 (0.02)
Acacia rigidula (3) (L)‡	0.91 (0.01)	0.06 (0.01)	0.03 (0.01)	0.79 (0.05)	0.21 (0.05)
All *Acacia*	0.90[a] (0.03)	0.07[b] (0.01)	0.03[c] (0.02)	0.87[d] (0.06)	0.13[ef] (0.06)
Quercus buckleyi (1)	0.88 (0.01)	0.07 (0.00)	0.06 (0.00)	0.88 (0.04)	0.12 (0.04)
Quercus gambelii (1)	0.89 (0.02)	0.07 (0.01)	0.05 (0.01)	0.87 (0.03)	0.13 (0.03)
Quercus pungens (2) (EG-S)	0.90 (0.01)	0.07 (0.01)	0.03 (0.01)	0.83 (0.02)	0.17 (0.02)
Quercus virginiana (2) (EG-S)	0.92 (0.00)	0.07 (0.00)	0.01 (0.00)	0.89 (0.03)	0.11 (0.03)
All *Quercus*	0.90[a] (0.02)	0.07[b] (0.00)	0.04[c] (0.02)	0.87[d] (0.05)	0.13[f] (0.05)
Acer negundo (1)	0.90 (0.01)	0.06 (0.01)	0.04 (0.01)	0.80 (0.03)	0.20 (0.03)
Berberis trifoliolata (3) (EG-NS)	0.90 (0.00)	0.06 (0.00)	0.04 (0.00)	0.85 (0.05)	0.15 (0.04)
Celtis reticulata (2)	0.89 (0.01)	0.07 (0.01)	0.05 (0.01)	0.87 (0.02)	0.13 (0.02)
Cercis canadensis (2) (L)	0.89 (0.00)	0.06 (0.00)	0.05 (0.00)	0.84 (0.02)	0.16 (0.02)
Colubrina texensis (2)	0.89 (0.01)	0.06 (0.01)	0.05 (0.01)	0.90 (0.01)	0.10 (0.01)
Condalia hookeri (3)	0.88 (0.01)	0.07 (0.01)	0.05 (0.01)	0.82 (0.02)	0.18 (0.02)
Diospyros texana (3)	0.92 (0.01)	0.06 (0.00)	0.02 (0.00)	0.82 (0.04)	0.18 (0.04)
Forestiera angustifolia (2)	0.87 (0.01)	0.08 (0.01)	0.06 (0.00)	0.84 (0.01)	0.16 (0.01)
Leucaena retusa (2) (L)	0.88 (0.01)	0.07 (0.01)	0.05 (0.00)	0.79 (0.06)	0.21 (0.06)
Lonicera albiflora (2)	0.89 (0.01)	0.06 (0.00)	0.05 (0.01)	0.86 (0.02)	0.14 (0.02)
Mahonia trifoliolata (3) (EG-S)	0.88 (0.00)	0.07 (0.00)	0.05 (0.00)	0.74 (0.01)	0.26 (0.01)
Morus microphylla (2)	0.89 (0.01)	0.06 (0.01)	0.05 (0.01)	0.88 (0.01)	0.12 (0.01)
Populus augustifolia (1)	0.91 (0.01)	0.05 (0.01)	0.04 (0.01)	0.84 (0.03)	0.16 (0.03)
Rhus aromatica (1)	0.90 (0.00)	0.06 (0.00)	0.04 (0.00)	0.92 (0.02)	0.08 (0.02)
Rhus microphylla (2)‡	0.90 (0.01)	0.06 (0.01)	0.04 (0.01)	0.85 (0.01)	0.15 (0.01)
Sophora secundiflora (2) (EG-S)	0.92 (0.00)	0.07 (0.00)	0.01 (0.00)	0.87 (0.02)	0.13 (0.02)
Ugnadia speciosa (2)	0.86 (0.01)	0.07 (0.01)	0.08 (0.01)	0.86 (0.03)	0.14 (0.03)
Zanthoxylum fagara (3) (EG-NS)	0.90 (0.01)	0.06 (0.00)	0.04 (0.01)	0.85 (0.02)	0.15 (0.02)
All trees/shrubs (n = 245)	0.90[a] (0.02)	0.07[b] (0.01)	0.04[c] (0.02)	0.85[d] (0.06)	0.15[f] (0.06)

Notes: Means are given with standard deviations in parentheses. Within each column, group means with different superscript letters were significantly different (t tests, $P < 0.05$). Locations of species are also marked: (1) Vernon, (2) Sonora, and (3) La Copita. For most species, n = 10; double dagger (‡) indicates n = 5. L = microphyllous legume, EG-S = evergreen sclerophyll, and EG-NS = evergreen nonsclerophyll. Tree/shrub species without notation were deciduous.

ume of most canopies throughout the greatest portion of a growing season.

Woody stem and standing litter optical properties

Woody plant stem and standing grass litter optical properties were generally more variable than those of fresh leaf material (Fig. 3). Coefficients of variation for stem reflectance ranged from 9 to 25% (highest in PAR region, lowest in SWIR near 1700 nm), while litter reflectance and transmittance CV's were 9–45% (lowest in NIR, highest in SWIR near 2400 nm) and 24–60% (lowest in NIR, highest in SWIR near 2400 nm), respectively. Among stem samples, this variability is probably attributable to differences in surface moisture and carbon constituents (Asner and Wessman 1997), although quantitative analyses of stem optical-biochemical relationships have not been adequately addressed. The wide range in grass litter optical properties may indicate differences in residual water content but also species-specific differences in carbon (e.g., lignin, cellulose, starch) content (Murray and Williams 1987, Asner, 1998). Woody stem and litter spectra showed fewer water absorption features than green leaf material, allowing the spectral features associated with lignin and other organic compounds (at ~1700, 2000, and 2200 nm) to emerge in the spectra (Curran et al. 1992, Verdebout et al. 1994, Asner et al. 1998*b*).

Upon convolving the spectra in the PAR range, we found variability in woody stem and litter absorptance to be greater than that of fresh leaves (Tables 2 and 3). The mean ± 1 SD absorptance for all woody stem and grass litter samples was 85 ± 6% and 67 ± 8%, respectively. Woody stem material absorbed PAR in quantities comparable to that of fresh leaf material. In fact, there were no statistically significant differences in PAR absorption between the mean fresh leaf (woody plant or grasses) and woody stem values.

North Texas savanna canopy structure

Diverse fire and grazing management histories, coupled with differences in long-term mean annual rainfall, combined to cause marked differences in tree and

TABLE 3. Variability of grass leaf and standing litter optical properties in the PAR spectral range.

Tissue	Species	Absorptance	Reflectance	Transmittance
Green leaves	*Agropyron cristatum* (2) (C_3)	0.88 (0.00)	0.09 (0.00)	0.03 (0.00)
	Aristida purpurea (1)	0.87 (0.01)	0.09 (0.01)	0.04 (0.01)
	Bothriochloa ischaemum (3)	0.86 (0.00)	0.11 (0.01)	0.04 (0.00)
	Bouteloua curtipendula (2)	0.87 (0.01)	0.10 (0.01)	0.04 (0.01)
	Bouteloua rigidiseta (1)‡	0.87 (0.01)	0.09 (0.01)	0.05 (0.01)
	Cenchrus ciliaris (3)‡	0.85 (0.01)	0.10 (0.01)	0.05 (0.01)
	Chloris pluriflora (3)	0.89 (0.00)	0.10 (0.01)	0.02 (0.00)
	Erioneuron pilosum (2)‡	0.90 (0.01)	0.08 (0.01)	0.02 (0.01)
	Paspalum spp. (3)	0.87 (0.01)	0.08 (0.01)	0.05 (0.01)
	Hilaria belangeri (2)‡	0.89 (0.00)	0.09 (0.00)	0.03 (0.00)
	Schizachyrium scoparium (2)	0.86 (0.01)	0.11 (0.01)	0.04 (0.01)
	Sorghastrum nutans (2)‡	0.88 (0.01)	0.09 (0.01)	0.03 (0.01)
	Stipa leucotricha (1) (C_3)	0.89 (0.01)	0.10 (0.01)	0.02 (0.01)
	Tripsacum dactyloides (2)	0.87 (0.00)	0.09 (0.00)	0.04 (0.00)
	All Grasses (n = 105)	0.87[a] (0.02)	0.10[c] (0.01)	0.04[e] (0.01)
Litter	*Agropyron cristatum* (C_3)	0.61 (0.05)	0.35 (0.04)	0.04 (0.02)
	Aristida purpurea	0.67 (0.04)	0.28 (0.05)	0.05 (0.03)
	Bothriochloa ischaemum	0.64 (0.06)	0.31 (0.04)	0.07 (0.02)
	Bouteloua curtipendula	0.59 (0.05)	0.33 (0.03)	0.09 (0.03)
	Bouteloua rigidiseta‡	0.69 (0.04)	0.25 (0.04)	0.08 (0.03)
	Cenchrus ciliaris‡	0.66 (0.05)	0.33 (0.04)	0.04 (0.02)
	Chloris pluriflora	0.68 (0.04)	0.26 (0.02)	0.07 (0.03)
	Erioneuron pilosum‡	0.74 (0.03)	0.23 (0.04)	0.03 (0.02)
	Hilaria belangeri‡	0.67 (0.07)	0.28 (0.03)	0.05 (0.02)
	Paspalum spp.	0.64 (0.05)	0.30 (0.04)	0.06 (0.03)
	Schizachyrium scoparium	0.56 (0.04)	0.31 (0.01)	0.16 (0.04)
	Sorghastrum nutans‡	0.62 (0.05)	0.36 (0.03)	0.03 (0.01)
	Stipa leucotricha (C_3)	0.58 (0.02)	0.32 (0.04)	0.10 (0.04)
	Tripsacum dactyloides	0.80 (0.01)	0.19 (0.02)	0.02 (0.01)
	All litter (n = 105)	0.67[b] (0.08)	0.28[d] (0.06)	0.07[e] (0.05)

Notes: Means are given with standard deviations in parentheses. Within each column, group means with different superscript letters are significantly different (t test, $P < 0.05$). Locations of species are also marked: (1) Vernon, (2) Sonora, and (3) La Copita. For most species, n = 10; double dagger (‡) indicates n = 5. C_3 = C_3 physiology. Grasses without notation have C_4 physiology.

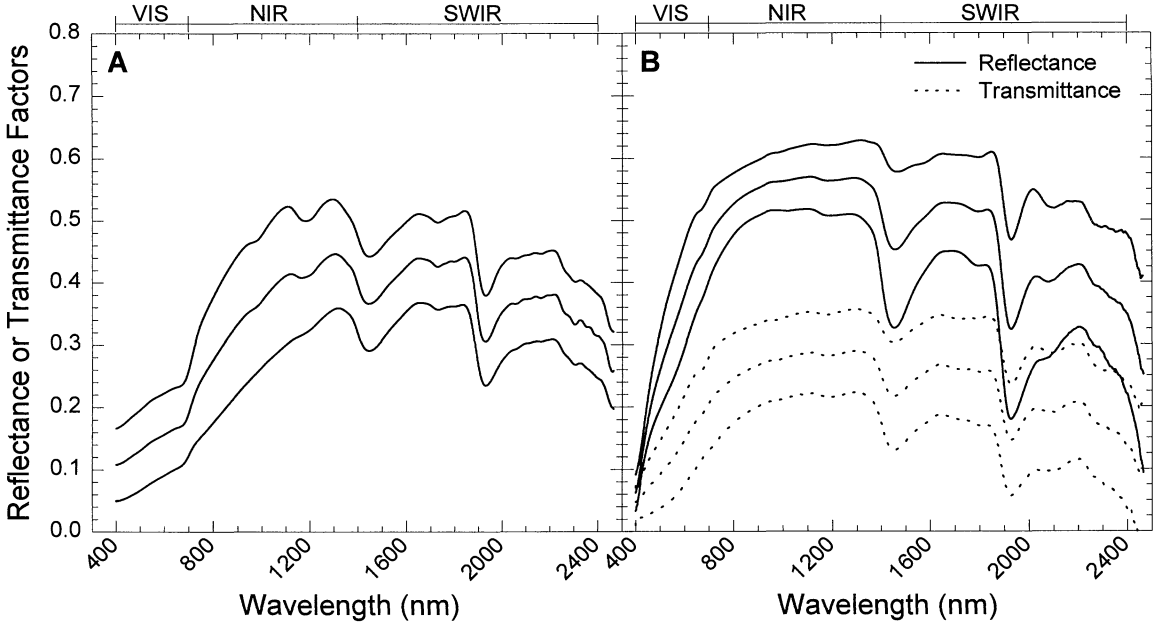

FIG. 3. Shortwave (400–2450 nm) stem reflectance (A) and litter reflectance and transmittance (B) for species collected along the north–south Texas savanna transect. Each set of three lines represents the mean ±1 SD. Visible (VIS), near-infrared (NIR), and shortwave-infrared (SWIR) spectral regions are indicated.

TABLE 4. Mean (1 SD in parentheses) leaf area index (LAI), plant area index (PAI = LAI + Litter AI), leaf and stem inclination angle (LA, SA), and tree crown dimensions for *Prosopis* and grass canopies in each 3600-m^2 plot at the North Texas savanna research site. Areal cover estimates of tree and herbaceous canopy and bare soils are also given.

	Tree					Grass		Ground cover
Plot	LAI (n = 15)	LA (°) (n = 300)	SA (°) (n = 30–60)	Crown height (m)† (n = 3)	Crown width (m)‡ (n = 3)	PAI (n = 30–36)	LA (°) (n = 180)	T/G/S§ (%)
1	1.1 (0.3)	43 (8)	58 (20)	2.9 (0.6)	4.9 (1.1)	3.6 (0.3)	50 (4)	44/87/13
2	2.1 (0.3)	38 (9)	68 (11)	2.5 (0.4)	2.7 (1.2)	3.8 (0.5)	49 (2)	53/93/7
3	1.5 (0.2)	41 (5)	49 (14)	3.0 (0.5)	3.0 (1.0)	2.8 (0.6)	51 (7)	51/98/2
4	1.3 (0.4)	37 (9)	69 (9)	2.6 (0.3)	2.6 (0.7)	2.6 (0.3)	57 (7)	42/98/2
5	2.2 (0.4)	41 (5)	74 (7)	3.7 (0.7)	5.9 (0.8)	2.3 (0.2)	50 (5)	55/88/12
6	1.8 (0.4)	41 (3)	50 (21)	3.0 (0.1)	3.5 (0.7)	3.3 (0.4)	48 (3)	34/97/3
7	2.0 (0.4)	37 (8)	72 (8)	3.0 (1.0)	4.1 (1.2)	3.0 (0.4)	52 (3)	45/96/4
8	1.4 (0.2)	45 (4)	63 (15)	3.6 (0.7)	4.2 (0.9)	3.1 (0.8)	48 (5)	39/97/3
9	1.9 (0.3)	42 (5)	79 (10)	3.7 (0.5)	4.0 (1.1)	3.9 (0.3)	49 (4)	34/98/2
10	1.9 (0.2)	41 (2)	73 (13)	4.9 (0.6)	5.2 (1.4)	4.4 (0.2)	56 (5)	41/97/3
Mean (SD)	1.7 (0.6)	41 (5)	66 (9)	3.3 (0.8)	4.2 (1.4)	3.2 (0.9)	54 (6)	T: 43.8 (7.4) G: 94.9 (4.2) S: 5.1 (4.2)
Min.	0.7	8	9	2.0	1.3	0.8	9	34/87/2
Max.	2.8	81	90	5.5	7.2	4.7	89	55/98/13

† Ground to crown top.
‡ Long axis.
§ T = tree, G = herbaceous, S = bare soil.

grass biomass between plots at the North Texas savanna site. Mean LAI ranged from 1.1 to 2.2 for *Prosopis* trees, while grass PAI (=LAI + Litter AI) varied from 2.3 to 4.4 (Table 4). Mean inclination angle of *Prosopis* leaflets ranged from 37° to 45° and that of grasses ranged from 48°to 57°. Our grass leaf angle values were similar to those reported for the tallgrass prairie in Kansas (Walter-Shea et al. 1992, Privette et al. 1996). The mean ± 1 SD *Prosopis* stem inclination angle was 66° ± 9°. Upon transforming the tissue angle data to distribution functions, we found that *Prosopis* leaf canopies tended toward plagiophile distributions (leaves distributed about a mean of 45°), while grass canopies and *Prosopis* stems tended toward erectophile distributions.

The mean ± 1 SD height (ground to top of crown) and width of *Prosopis* was 3.3 ± 0.8 and 4.2 ± 1.4 m, respectively. *Prosopis* stem area index (SAI) ranged from 0.44 to 0.66. When samples were separated into canopy height classes, mean ± 1 SD SAI values for the 0.5–1.0, 1.0–2.0, and >2.0 m classes were 0.50 ± 0.35, 0.48 ± 0.25, and 0.62 ± 0.20, respectively. The relative proportion of leaf to stem area (~2.0–4.5) was comparable to that in the few studies that have measured both LAI and SAI (O'Connell and Kelty 1994; D. Pataki, Duke University, *personal communication*). These LAI, SAI, and leaf angle results provided the necessary range of structural values to test the canopy radiative transfer model.

Air photo analyses of the North Texas site indicated that the areal extent of tree cover ranged from 34 to 55% with a mean value of 44% (Table 4). Grass cover was estimated as the reciprocal amount of understory cover not classified as bare soil. This approach makes the assumption that grass cover was present under tree crowns (which cannot be estimated from aerial photographs), and field observations supported this assumption for the North Texas sites. Grass and bare soil cover ranged from 87 to 98 and from 2 to 13%, respectively.

Radiative transfer model evaluation

Field measurements of canopy PAR interception (fIPAR) were regressed against model predictions for *Prosopis* trees and grass plots. For the tree canopy simulations, a mean SAI of 0.55 was used. Scattering by leaves, stems, and litter was parameterized using mean reflectance and transmittance values for *Prosopis* and grass species located at the North Texas site (Tables 2 and 3). Tree leaf and woody stem angle distributions (LAD, SAD) were modeled as plagiophile and erectophile, respectively. Grass leaf and standing litter angle distributions were both simulated as erectophile. For *Prosopis* trees, the index of foliage clumping was set at 0.8 to simulate a moderate amount of clumping (Qin 1993). This parameter was difficult to quantify in the field, so we chose a value to best represent our qualitative field observations.

Radiative transfer model predictions of *Prosopis* fIPAR were in close agreement with field measurements (r^2 = 0.97), and absolute errors ranged from 0 to 4% (Fig. 4A). Predictions of fIPAR in grass plots were reasonably accurate (r^2 = 0.87; Fig. 4B), but were significantly improved when the model was parameterized with both grass leaf and litter optical properties (r^2 = 0.94; Fig. 4C). This improvement was accom-

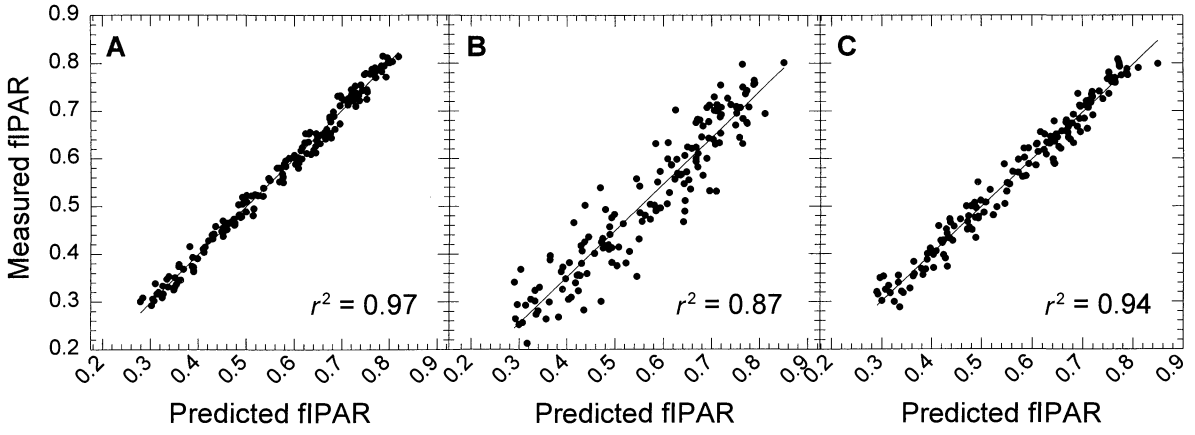

FIG. 4. Observed fIPAR (fraction of photosynthetically active radiation intercepted) vs. that predicted from the canopy radiative transfer model parameterized for the north Texas savanna site for (A) *Prosopis* canopies, (B) grass canopies without taking litter into account, and (C) grass canopies after weighting the modeled canopies with field estimates of litter cover.

plished by weighting each simulated plot using the field estimates of live and dead grass cover. Strong agreement between predicted and observed fIPAR for tree and grass canopies indicated that we could reliably proceed with sensitivity analyses to determine the relative importance of the leaf, stem, and litter optical properties on canopy fAPAR.

Determinants of canopy PAR absorption

For canopy-level sensitivity analyses, vegetation and soil parameter values are listed in Table 5 (column 1) unless noted otherwise. Using the measured variability in leaf-level reflectance and transmittance values (Tables 2 and 3), we first considered the influence of their scattering properties on canopy-level fAPAR. We began by simulating a tree canopy consisting of leaves without stems, as is commonly done in canopy radiation modeling. Varying leaf optical properties ± 2 SD from the mean had little influence on canopy fAPAR (Fig. 5A). At LAI < 2, the effect of changing leaf optical properties was insignificant. At high LAI values (5–6), leaf optical variability affected canopy fAPAR by only 5–6% (absolute).

Adding woody stem optical properties and woody stem area to the model (Table 5) increased canopy fAPAR by 10–40% (absolute) at LAI < 3, with a diminishing influence as LAI increased to 6 (Fig. 5B). Varying stem optical properties by ±2 SD from the mean in Table 3 had a minimal (<6%) effect on canopy fAPAR, regardless of LAI or SAI. Thus, while nonphotosynthetic woody plant components contribute significantly to canopy fAPAR, variation in their optical properties was of little consequence.

An analogous series of simulations was performed for grass canopies to test the relative importance of live foliage and standing litter on canopy fAPAR. Using the measured variation in grass leaf and litter optical properties, we compared a simulated 100% live leaf canopy to a mixed (50% live/50% litter) canopy (Fig. 6A). As was observed for simulated tree canopies, the importance of leaf scattering characteristics (±2 SD from the mean) increased as canopy PAI increased. However, even at very high PAIs (5–6), grass leaf optical properties accounted for <3% of the variation in canopy fAPAR. The mixed live/litter grass canopies showed a similar trend, but the greater variation in litter reflectance and transmittance (Table 3) translated to larger differences in canopy-level fAPAR as PAI increased (Fig. 6A). Note that even at a high canopy PAI, the difference between live only and live + litter canopy fAPAR was only 4–7%.

To further examine the importance of leaf and standing litter contributions to grass canopy fAPAR, we simulated five canopy PAI scenarios, where the amount of live material ranged from 0 to 100% (Fig. 6B). Canopy fAPAR was driven primarily by the total amount of biomass (live + litter) present, with the proportion of live vs. dead leaf material playing a relatively small role. As the live leaf proportion increased for any given PAI, canopy fAPAR increased linearly, with a maximum change of ~8% from a 100% litter to a 100% live canopy. Thus, for every 20% increase in live material, canopy fAPAR increased by <2%.

Determinants of landscape PAR absorption

We used the PCA approach described earlier to quantify the relative importance of the various tissue optical properties and tree cover, LAI, and SAI to landscape fAPAR in relation to changes in the sum of component (tree and grass) canopy LAIs (called the "sum component LAI"). The *y*-axis in Fig. 7 shows the effect of a 10% change in a given leaf-, canopy-, or landscape-level variable on total landscape fAPAR. For example, with a tree canopy LAI = 0.5 and a sum component LAI = 1.5 (grass LAI = 1.0 + tree LAI = 0.5), a 10% change in the relative cover of trees accounted for a

TABLE 5. Leaf- to landscape-level parameters used for radiative transfer sensitivity analyses.

Parameters	Values for canopy-level analyses	Values for landscape-level analyses
Leaf level		
Hemispherical reflectance (400–700 nm)		
Arborescent species	0.07	0.04–0.10
Grass species	0.10	0.06–0.14
Stem material	0.15	0.05–0.28
Litter	0.28	0.16–0.40
Hemispherical transmittance (400–700 nm)		
Arborescent species	0.04	0.01–0.09
Grass species	0.04	0.1–0.08
Stem material	0.00	0.00
Litter	0.07	0.02–0.20
Canopy level		
Overstory leaf area index	0.0–5.0	0.0–5.0
Overstory stem area index	0.55, 0.65	0.0–1.0
Understory leaf area index	0.0–5.0	0.5, 1.0, 2.5
Understory litter area index	0.0–5.0	0.5, 1.0, 2.5
Soil reflectance	0.15†	0.15†
Overstory leaf angle	plagiophile	plagiophile
Understory leaf angle	erectophile	erectophile
Overstory stem angle	erectophile	erectophile
Understory litter angle	erectophile	erectophile
Landscape level		
Areal coverage of overstory	n/a	0–100%
Overstory crown height (m)	3.3	3.3
Overstory crown diameter (m)	4.2	4.2
Understory canopy height (m)	0.4	0.4
Other		
Ratio of direct to total incident radiation	0.8	0.8
Solar zenith angle	15°	15°

Note: Value means and ranges in Tables 2 and 3 were used for setting leaf, stem, and litter optical properties. All other values were from the North Texas savanna site or were chosen within ecologically plausible limits. Middle column shows baseline values used for canopy-level analyses (Figs. 5 and 6); n/a indicates not applicable. Far right column indicates ranges of values used in landscape sensitivity analyses (Figs. 7 and 8). Plagiophile = distribution of leaf zenith angle tends toward 45°. Erectophile = distribution of leaf zenith angle tends toward vertical.

† From Asner and Wessman (1997).

8% change in total landscape fAPAR (Fig. 7A). Under these same conditions, a 10% change in tree LAI accounted for 55% of the change in landscape fAPAR.

Tree LAI and tree cover clearly controlled the variance in landscape-level fAPAR. These variables combined to account for 60–80% of the PCA variance in fAPAR (Fig. 7A), whereas stem area index and tissue optical properties combined to account for 20–40% of the variance (Fig. 7B). The importance of tree cover increased as the sum component LAI increased, with a concomitant decline in the importance of tree canopy LAI. One of these two variables explained ≥40% of the variance in landscape fAPAR, whereas stem area index and tissue optical properties never accounted for more than ~11% when considered individually. Among these secondary variables, stem area index exerted more influence than most tissue optical properties. However, its importance, as well as the importance of grass and litter optical properties, decreased with increasing sum component LAI (Fig. 7B). Conversely, tree leaf optical properties increased in importance with increasing tree LAI. The optical properties of standing litter was of similar importance to that of live grass in driving fAPAR variability at all sum component LAI values.

In the previous analysis, the understory herbaceous cover was held constant with a live/standing litter mixture PAI = 2.0 (each understory component = 1.0). To further test the relative importance of tree cover and LAI on fAPAR when understory conditions change, we simulated landscape fAPAR for two live grass (LAI = 0.5, 2.5) and four tree (LAI = 1.0, 2.0, 3.0, 4.0) scenarios, while increasing tree canopy cover from 10 to 90%. Landscape fAPAR increased with added tree cover, but the influence of tree canopy leaf area on landscape fAPAR diminished when the understory LAI was relatively high (Fig. 8). This supports other work indicating that absorption in the PAR region saturates at moderate LAI (2–3) values (e.g., Asrar et al. 1984, Goward and Huemmrich 1992). As a result, adding tree

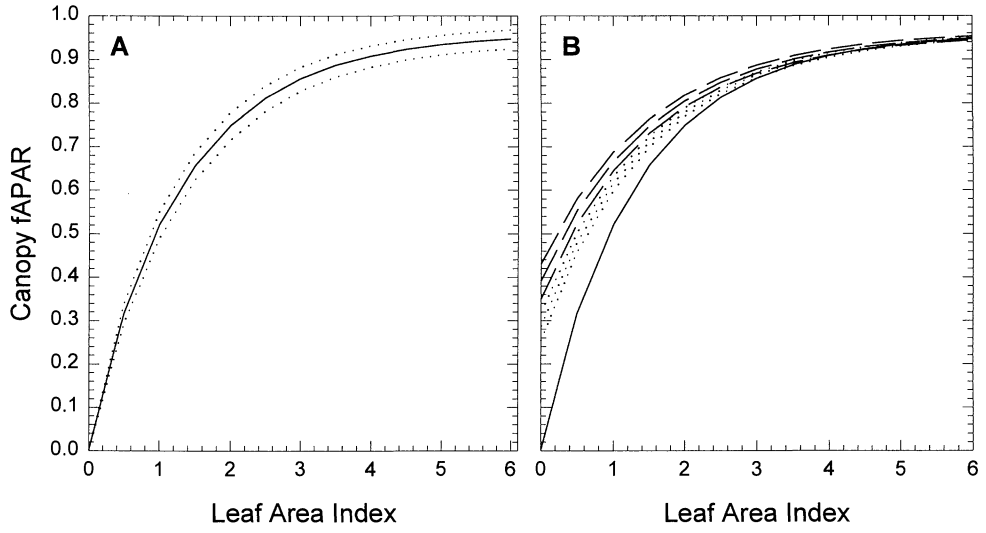

FIG. 5. (A) Relative importance of the measured variability in leaf optical properties on woody plant canopy fAPAR (fraction of photosynthetically active radiation absorbed). Solid line shows the change in canopy fAPAR with increasing LAI using the mean leaf-level reflectance and transmittance values from Table 2. Dotted lines depict ±2 SD. (B) Role of measured variability in stem area and stem optical properties for arborescent (e.g., *Prosopis glandulosa*) canopies. Solid (lower) line shows the same relationship as in (A) when stem material is absent. Dotted lines depict the mean (±2 SD in stem optical properties) canopy fAPAR values after incorporating a stem area index of 0.45 (from field measurements). Dashed (upper) lines are the same, but with the stem area index value set to 0.65 (the upper limit of field observations).

LAI when understory LAI is already high produced only small (<5%) changes in fAPAR at the landscape level (Fig. 8B), whereas in the low understory LAI case, incremental changes in tree canopy LAI increased landscape fAPAR as much as 25% (Fig. 8A). In the low grass LAI simulation (Fig. 8A), a tree cover of 80–90% was required to generate a landscape-level fAPAR comparable to that of a nearly treeless (~10% tree cover) grassland with an LAI = 2.5.

A similar set of analyses, but with an understory composed of 100% standing litter (Litter AI = 0.5, 2.5) showed trends comparable to those observed for green grass canopies (Fig. 8c, d). While landscape fAPAR was slightly lower in comparison to the scenarios with a green understory (Fig. 8A, B), the differences were <7% (absolute). As the extent and LAI of the overstory increased, the differences in landscape fAPAR between the live and senescent understory scenarios decreased to almost zero.

DISCUSSION

Understanding and quantifying the determinants of PAR absorption by plant canopies are critical for ac-

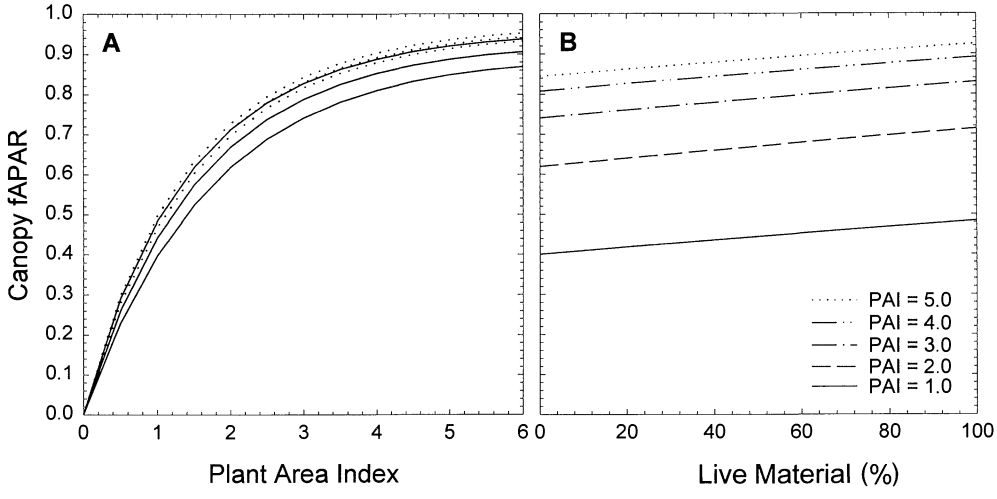

FIG. 6. (A) Dotted lines depict fAPAR with increasing PAI (plant area index) for live grass canopies using mean grass leaf optical values (±2 SD; Table 3). Solid lines depict a canopy composed of 50% live/50% senescent (litter) material (mean ±2 SD of leaf and litter optical properties). (B) Effect of increasing the percentage of live material on grass canopy fAPAR at five canopy PAI values. Changes in live:litter ratios had less effect on canopy fAPAR than changes in canopy PAI.

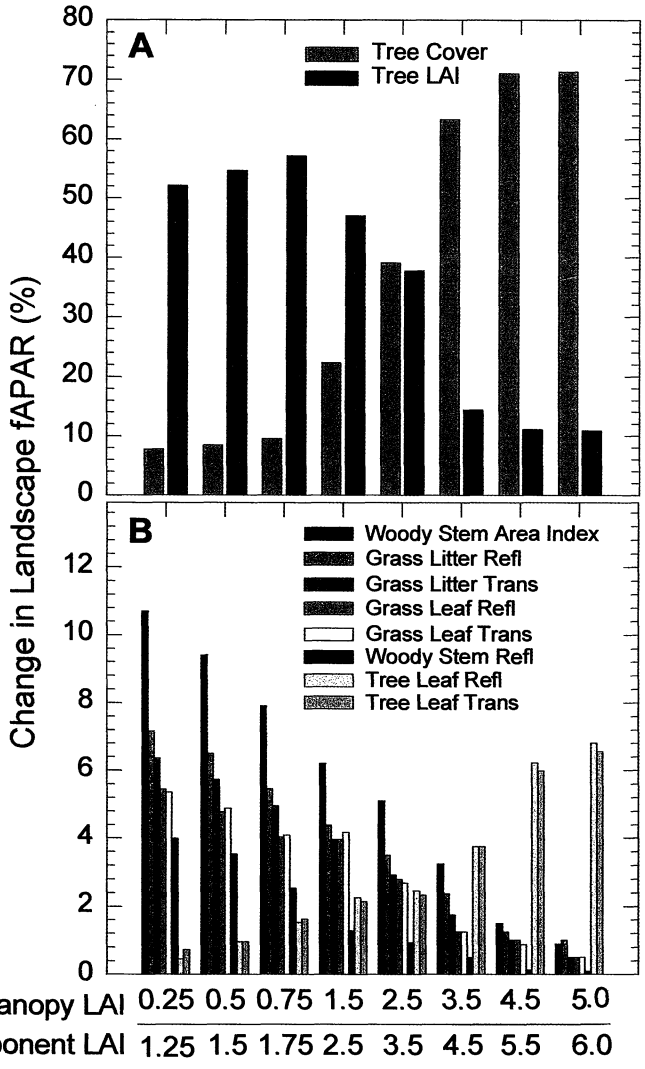

FIG. 7. Savanna landscape fAPAR sensitivity results. For this analysis, the x-axes show changes in tree canopy LAI or changes in the sum of tree and grass landscape component LAI (holding grass PAI = 2.0 with LAI = 1.0/Litter AI = 1.0). The y-axis represents the proportion of landscape fAPAR variance accounted for by a given variable. (A) Variation in fractional tree cover and tree canopy LAI combined to account for 60–80% of the variance in landscape fAPAR, but their relative importance shifts with increasing sum component LAI. (B) Stem area index and tissue optical properties combined to account for 20–40% of the variance in landscape fAPAR, but no single variable accounted for >11%. The importance of stem area index decreases and that of tree leaf optical properties increases with increasing sum component LAI. The contribution of litter meets or exceeds that of green grass at all LAI values.

curate modeling of canopy carbon, water, and trace gas fluxes (e.g., Collatz et al. 1991, Baldocchi 1993). Although studies based on light attenuation in forest canopies appear to provide adequate resolution for these applications, they may not apply well to canopies with gaps, a relatively large proportion of nonphotosynthetic material (e.g., stems), vertical layering of vegetation types, or in areas of high horizontal heterogeneity. Furthermore, statistical light attenuation models, such as those based solely on the Poisson probability distribution (Nilson 1971), do not provide a means to quantify the relative importance of the scaled biophysical and structural variables that determine canopy and landscape PAR absorption.

Radiative transfer models based on physical scattering principles provide a means to evaluate the relative importance of variables contributing to the canopy radiation regime. We first quantified the optical characteristics of a wide array of leaf, woody stem, and standing litter components, the smallest-scale elements in most radiative transfer models (but see Jacquemoud and Baret [1990] for an example of within-leaf modeling), to define the limits of their scattering properties. Because these models provide a means to link tissue-

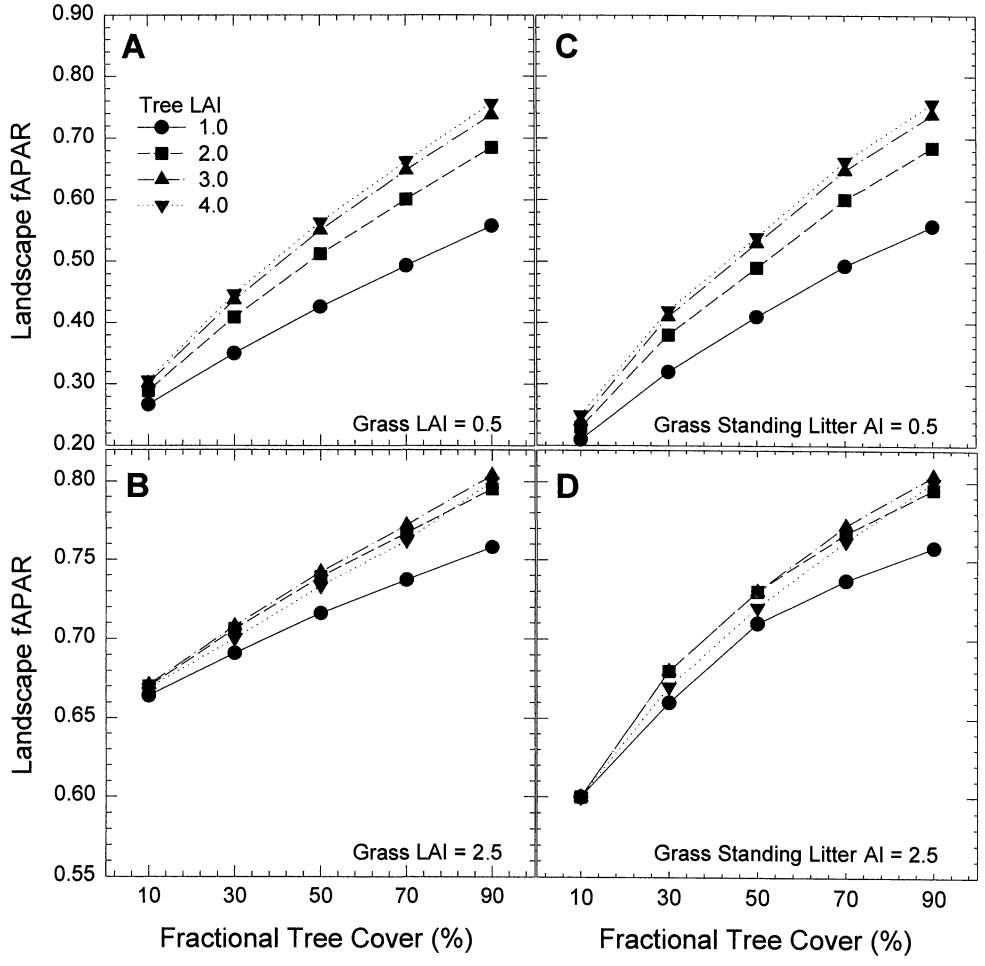

FIG. 8. (A) Effect of changing tree cover on landscape fAPAR for four tree canopy LAI scenarios when the understory is composed of a grass canopy with LAI = 0.5. When understory LAI was low, changes in overstory cover and LAI had significant effects on landscape fAPAR. (B) For a high understory LAI = 2.5 scenario, changes in tree cover or tree canopy LAI had little effect on landscape fAPAR. Note the difference in *y*-axes between panels (A) and (B). (C, D) Same as (A) and (B) but with an understory canopy composed of 100% standing litter. Trends similar to those observed for live grass canopies emerged and illustrate that litter canopies absorb significant amounts of PAR.

scattering characteristics to the canopy structural attributes determining the abundance, position, and orientation of scattering objects in three-dimensional space, canopy absorption of photons can be simulated in a highly mechanistic manner. This approach thus lent itself well to quantitative analyses.

Our results indicate that variation in woody plant and grass leaf optical properties accounts for only a small proportion of the variance in canopy-level fAPAR. Changes in canopy fAPAR resulting from changes in LAI far outweighed those associated with changes in leaf scattering characteristics. For canopy-scale assessments of light absorption, it thus appears that leaf optical properties in the PAR spectral region can be treated generically. The greater observed variability in the scattering characteristics of leaves in the NIR and SWIR spectral regions (Figs. 2 and 3) would likely preclude the use of generic leaf optical properties in radiation budget studies focused on the entire shortwave spectrum (e.g., for albedo studies).

Woody stem material absorbed significant amounts of PAR and substantially increased canopy fAPAR at a low to moderate LAI. Senescent biomass also strongly absorbed PAR. As a result, an accounting of stem area in woody plants and the relative proportion of live and standing litter cover in herbaceous canopies is necessary to accurately model ecophysiological processes at the canopy scale in grasslands, savannas, shrublands, and woodlands. It is the "functional fAPAR," i.e., the absorbed PAR used in photosynthesis, that is needed in such modeling efforts. Studies seeking to quantify canopy photosynthesis, respiration, and trace gas dynamics would likely incorporate significant error from functional fAPAR estimates based solely on whole-

canopy field measurements. Even at relatively high LAI values, ecophysiological analyses that neglect contributions from stem and senescent leaf surfaces to canopy fAPAR introduce a bias in flux estimates that could be magnified when extrapolated over increasingly large regions (Asner and Wessman 1997).

These results emphasize that senescent grass canopies absorb photosynthetically active radiation in quantities similar to those of live grass canopies, although the amount that goes to "functional fAPAR" will decrease with increasing canopy senescence. This counterintuitive outcome occurs because increased scattering in a standing litter canopy allows photons to travel more deeply into the canopy and thus maintain overall canopy fAPAR (Fig. 6B) by offsetting the greater reflectance of senescent grass material at the top of the canopy (Table 3). The remaining difference between green leaf and standing litter canopy fAPAR at any given plant area index (PAI) was primarily the result of scattering losses at the top of the canopy (results not shown).

At landscape scales, variation in PAR absorption was largely driven by changes in the spatial extent and PAI of vegetation types. When considered individually, woody stem area and scattering characteristics of leaves, stems, and litter contributed little to landscape-level fAPAR. However, as a group, these variables did combine to account for 20–40% of the variance in landscape fAPAR, and thus, should not be ignored. This landscape analysis provides quantitative information regarding which variables could be treated generically or ignored in analyses of ecosystem function. For example, in low PAI environments (e.g., arid shrublands), changes in PAI and the amount and optical properties of nonphotosynthetic vegetation (NPV) components play a significant role in determining landscape fAPAR. Fresh leaf optical properties play a very small role. In high PAI situations (e.g., forests), canopy gap fraction (analogous to tree cover) and leaf optical properties play a more important role, while other factors, such as NPV, might be ignored. Nonetheless, caution in applying these results to forested ecosystems should be exercised since functional processes in the upper reaches of a canopy (e.g., where cumulative LAI < 3.0) can be influenced by the presence of woody material.

Although soil optical properties were not explicitly addressed in this study, other analyses have indicated that soil reflectance does influence canopy fAPAR (e.g., Asrar et al. 1992, Asner and Wessman 1997). However, bare ground cover at our North Texas savanna site was only 2–13% (Table 4), and even where large bare soil patches occur, variation in vegetation cover and LAI are the primary determinants of landscape-level PAR absorption (Asrar et al. 1992). Leaf angle distribution is also an important factor controlling fAPAR (e.g., Asrar et al. 1992, Walter-Shea et al. 1992, Norman 1993, and many others). Our approach was to quickly survey leaf and stem angle distributions at our savanna site and use these data to realistically parameterize the radiative transfer model. In other analyses, Asner and Wessman (1997) indicated the role of leaf angle distribution in driving fAPAR variability as intermediate to that of LAI and some of the secondary factors described in Fig. 7, such as stem area.

Conclusions

Results of this study provide quantitative insights to the relative importance of several scale-dependent factors influencing fAPAR in grass and woody plant canopies in spatially heterogeneous landscapes. fAPAR is of particular importance because it provides a direct connection between ecosystem structure and function (Wessman and Asner 1998). It also provides a means to link repeatable, synoptic-scale remote sensing estimates of fAPAR to other functional attributes of ecosystems such as nitrogen use, CO_2 assimilation, and water loss (Sellers 1987, Sellers et al. 1992, Running et al. 1994, Field et al. 1995). While fAPAR is a functional attribute of an ecosystem, it is strongly influenced by ecosystem structure (e.g., Gamon et al. 1995). As a result, deconvolving the relative effects of the numerous structural factors that control fAPAR is needed to improve its interpretation and use. The importance of many single factors contributing to canopy fAPAR has been documented in previous studies. Here, we demonstrated their relative significance at the scale of tissues, canopies, and landscapes as a means to determine which variables should be accounted for and which can be ignored or held to a constant value in future studies. Further analyses are underway to incorporate this understanding of fAPAR scale dependence into the interpretation of remotely sensed data.

Improved accuracy in scaling biophysical variables will continue to be important for both bottom-up and top-down perspectives in physiological ecology, biogeochemistry, and global change research. Studies focused on large-scale ecological change, such as the interaction of the biosphere and atmosphere through CO_2 and water vapor exchange, require improved resolution in space and time, and improved functional links to landscape-, regional-, and global-scale structural heterogeneity. As new perspectives and methods for scaling ecological function from local to global levels continue to evolve (e.g., via micrometeorological towers, remote sensing, and modeling), our understanding of how observable functional variables (e.g., fAPAR) scale across ecological levels must keep pace. Without this synergy, our ability to resolve important issues such as sources and sinks of CO_2, the effects of nitrogen deposition on ecosystems, and the significance of land-use and climate change will be impaired.

Acknowledgments

We greatly appreciate the field assistance provided by Sam Fuhlendorf, Alan Townsend, and Steven Zitzer. Many thanks go to Ranga Myneni for providing much of the modeling

code and advice on canopy photon transport modeling; this study could not have been completed without Dr. Myneni's help. Jim Ansley and Julie Huddle provided valuable logistical support. Casey Cody provided air photo processing and interpretation. Alan Townsend provided extremely helpful comments on the manuscript. We also appreciate the kind help and warm welcome received from many people at the Texas A&M Vernon, Sonora, and La Copita Research and Extension Centers. This work was supported by NASA Innovative Research Grant NAGW-4689, NASA EOS Interdisciplinary Science Award NAGW-2662, and a NASA Earth System Science Fellowship Award to G. P. Asner.

Literature Cited

Amos, B. B., and F. R. Gehlbach. 1988. Edwards Plateau vegetation. Baylor University Press, Waco, Texas, USA.

Archer, S. 1994. Woody plant encroachment into southwestern grasslands and savannas: rates, patterns and proximate causes. Pages 13–68 *in* M. Vavra, W. A. Laycock, and R. D. Pieper, editors. Ecological implications of livestock herbivory in the West. Society for Range Management, Denver, Colorado, USA.

———. 1995. Tree-grass dynamics in a Prosopis-thornscrub savanna parkland: reconstructing the past and predicting the future. Ecoscience **2**:83–99.

Asner, G. P. 1998. Biophysical and biochemical sources of variation in canopy reflectance. Remote Sensing of Environment **64**:234–253.

Asner, G. P., B. H. Braswell, D. S. Schimel, and C. A. Wessman. 1998*a*. Ecological research needs from multi-angle remote sensing data. Remote Sensing of Environment **63**: 155–165.

Asner, G. P., and C. A. Wessman. 1997. Scaling PAR absorption from the leaf to landscape level in spatially heterogeneous ecosystems. Ecological Modelling **101**:145–163.

Asner, G. P., C. A. Wessman, D. S. Schimel, and S. Archer. 1998*b*. Variability in leaf and litter optical properties: implications for BRDF model inversions using AVHRR, MODIS, and MISR. Remote Sensing of Environment **63**: 200–215.

Asrar, G., M. Fuchs, E. T. Kanemasu, and M. Yoshida. 1984. Estimating absorbed photosynthetic radiation and leaf area index from spectral reflectance in wheat. Agronomy Journal **76**:300–306.

Asrar, G., R. B. Myneni, and B. J. Choudhury. 1992. Spatial heterogeneity in vegetation canopies and remote sensing of absorbed photosynthetically active radiation: a modeling study. Remote Sensing of Environment **41**:85–103.

Baldocchi, D. D. 1992. A Lagrangian random-walk model for simulating water vapor, CO_2, and sensible heat flux densities and scalar profiles over and within a soybean canopy. Boundary-layer Meteorology **61**:113–127.

———. 1993. Scaling water vapor and carbon dioxide exchange from leaves to a canopy: rules and tools. Pages 77–116 *in* J. R. Ehleringer and C. B. Field, editors. Scaling physiological processes: leaf to globe. Academic Press, New York, New York, USA.

Baldocchi, D. D., and B. A. Hutchinson. 1986. On estimating canopy photosynthesis and stomatal conductance in a deciduous forest with clumped foliage. Tree Physiology **2**: 155–165.

Boyer, M., J. Miller, M. Belanger, E. Hare, and J. Wu. 1988. Senescence and spectral reflectance in leaves in northern pin oak (*Quercus palustris* Muenchh.). Remote Sensing of Environment **25**:71–87.

Campbell, G. S. 1986. Extinction coefficients for radiation in plant canopies calculated using an ellipsoidal inclination angle distribution. Agricultural Forest Meteorology **36**: 317–321.

Ciais, P., P. P. Tans, M. Trolier, J. W. C. White, and R. J. Francey. 1995. A large Northern Hemisphere terrestrial CO_2 sink indicated by the $^{13}C/^{12}C$ ratio of atmospheric CO_2. Science **269**:1098–1102.

Collatz, G. J., J. T. Ball, C. Grivet, and J. A. Berry. 1991. Physiological and environmental regulation of stomatal conductance, photosynthesis, and transpiration: a model that includes a laminar boundary layer. Agricultural Forest Meteorology **54**:107–136.

Crutzen, P. J., and M. O. Andreae. 1990. Biomass burning in the tropics: impact on atmospheric chemistry and biogeochemical cycles. Science **250**:1669–1678.

Curcio, J. A., and C. C. Petty. 1951. Extinction coefficients for pure liquid water. Journal of the Optical Society of America **41**:302–312.

Curran, P. J., J. L. Dungan, B. A. Macler, S. E. Plummer, and D. L. Peterson. 1992. Reflectance spectroscopy of fresh whole leaves for the estimation of chemical concentration. Remote Sensing of Environment **39**:153–166.

Danks, S. M., E. H. Evans, and P. A. Whittaker. 1984. Photosynthetic systems: structure, function and assembly. Wiley, New York, New York, USA.

Daugherty, C. S. T., K. J. Ranson, and L. L. Biehl. 1989. A new technique to measure the spectral properties of conifer needles. Remote Sensing of Environment **27**:81–91.

Denning, A. S., I. Y. Fung, and D. Randall. 1995. Latitudinal gradient in atmospheric CO_2 due to seasonal exchange with the land biota. Nature **376**:240–242.

Ehleringer, J., and R. W. Pearcy. 1983. Variation in quantum yield for CO_2 uptake among C_3 and C_4 plants. Plant Physiology **73**:555–559.

Field, C. B., J. T. Randerson, and C. M. Malmstrom. 1995. Global net primary production: combining ecology and remote sensing. Remote Sensing of Environment **51**:74–88.

Florian, J., S. J. Milton, W. R. J. Dean, and N. Van Rooyen. 1996. Tree spacing and coexistence in semiarid savannas. Journal of Ecology **74**:583–595.

Fourty, Th., F. Baret, S. Jacquemoud, G. Schmuck, and J. Verdebout. 1996. Leaf optical properties with explicit description of its biochemical composition: direct and inverse problems. Remote Sensing of Environment **56**:104–117.

Gamon, J. A., C. B. Field, M. L. Goulden, K. L. Griffin, A. E. Hartley, G. Joel, J. Penuelas, and R. Valentini. 1995. Relationships between NDVI, canopy structure, and photosynthesis in three Californian vegetation types. Ecological Applications **5**:28–41.

Gao, B.-C., and A. F. H. Goetz. 1995. Retrieval of equivalent water thickness and information related to biochemical components of vegetation canopies from AVIRIS data. Remote Sensing of Environment **52**:155–162.

Gates, D. M., H. J. Keegan, J. C. Schleter, and V. R. Wiedner. 1965. Spectral properties of plants. Applied Optics **4**:11–20.

Gausman, H. W. 1982. Visible light reflectance, transmittance, and absorptance of differently pigmented cotton leaves. Remote Sensing of Environment **13**:233–238.

Goward, S. N., and K. F. Huemmrich. 1992. Vegetation canopy PAR absorptance and the normalized difference vegetation index: an assessment using the SAIL model. Remote Sensing of Environment **39**:119–140.

Heitschmidt, R. K., R. D. Schultz, and C. J. Scifres. 1986. Herbaceous biomass dynamics and net primary production following chemical control of honey mesquite. Journal of Range Management **39**:67–71.

Horler, D. N. H., M. Dockray, and J. Barber. 1983. The red edge of plant leaf reflectance. International Journal of Remote Sensing **4**:273–278.

Jacquemoud, S., and F. Baret. 1990. PROSPECT: a model of leaf optical properties spectra. Remote Sensing of Environment **34**:75–91.

Jacquemoud, S., F. Baret, and J. F. Hanocq. 1992. Modeling

spectral and bidirectional soil reflectance. Remote Sensing of Environment **41**:123–132.

Kuusk, A. 1995. A fast, invertible canopy reflectance model. Remote Sensing of Environment **51**:342–350.

Lee, D. W., and R. Graham. 1986. Leaf optical properties of rainforest sun and extreme shade plants. American Journal of Botany **73**:1100–1108.

Li, X., and A. H. Strahler. 1985. Geometric-optical modeling of a coniferous forest canopy. IEEE Transactions on Geoscience and Remote Sensing **23**:207–221.

LI-COR. 1992. LAI-2000 plant canopy analyzer operating manual. LI-COR, Inc., Lincoln, Nebraska, USA.

Liang, S., and A. H. Strahler. 1993. An analytic BRDF model of canopy radiative transfer and its inversion. IEEE Transactions on Geoscience and Remote Sensing **31**:1081–1095.

Maas, S. J., and J. R. Dunlap. 1989. Reflectance, transmittance, and absorptance of light by normal, etiolated, and albino corn leaves. Agronomy Journal **81**:105–110.

Marshak, A. L. 1989. The effect of the hot spot on the transport equation in plant canopies. Journal of Quantitative Spectroscopy and Radiative Transfer **42**:615–630.

Matthews, E. 1983. Global vegetation and land-use: new high-resolution databases for climate studies. Journal of Applied Meteorology **22**:474–487.

Middleton, E. M., S. S. Chan, M. A. Mesarch, and E. A. Walter-Shea. 1996. A revised methodology for spectral optical properties of conifer needles. IGARSS 96 Digest **2**:1005–1009.

Murray, I., and P. C. Williams. 1987. Chemical principles of near-infrared technology. Pages 17–34 *in* P. Williams and K. Norris, editors. Near-infrared technology in the agricultural and food industries. American Association of Cereal Chemists, St. Paul, Minnesota, USA.

Myneni, R. B., and G. Asrar. 1993. Radiative transfer in three-dimensional atmosphere-vegetation media. Journal of Quantitative Spectroscopy and Radiative Transfer **49**:585–598.

Myneni, R. B., J. Ross, and G. Asrar. 1989. A review on the theory of photon transport in leaf canopies. Agricultural Forest Meteorology **45**:1–153.

Nilson, T. 1971. A theoretical analysis of the frequency of gaps in plant stands. Agricultural Forest Meteorology **8**: 25–38.

Norman, J. M. 1979. Modeling the complete crop canopy. Pages 249–277 *in* B. J. Barfield and J. F. Gerber, editors. Modification of the aerial environment of plants. American Society of Agricultural Engineers, St. Joseph, Michigan, USA.

———. 1993. Scaling processes between leaf and canopy levels. Pages 41–76 *in* J. R. Ehleringer and C. B. Field, editors. Scaling physiological processes: leaf to globe. Academic Press, New York, New York, USA.

O'Connell, B. M., and M. J. Kelty. 1994. Crown architecture of understory and open-grown white pine (*Pinus strobus* L.) saplings. Tree Physiology **14**:89–97.

Poorter, L., S. F. Oberbauer, and D. B. Clark. 1995. Leaf optical properties along a vertical gradient in a tropical rain forest canopy in Costa Rica. American Journal of Botany **82**:1257–1263.

Prince, S. D. 1991. A model of regional primary production for use with course resolution satellite data. International Journal of Remote Sensing **12**:1313–1330.

Privette, J. L., W. J. Emery, and D. S. Schimel. 1996. Inversion of a vegetation reflectance model with NOAA AVHRR data. Remote Sensing of Environment **46**:235–245.

Qin, W. 1993. Modeling bidirectional reflectance of multi-component vegetation canopies. Remote Sensing of Environment **46**:235–245.

Ross, J. K. 1981. The radiation regime and architecture of plant stands. Kluwer Boston, Hingham, Massachusetts, USA.

Running, S. W., T. R. Loveland, and L. L. Pierce. 1994. A vegetation classification logic based on remote sensing for use in global biogeochemical models. Ambio **23**:77–89.

Russell, G., P. G. Jarvis, and J. L. Monteith. 1989. Absorption of radiation by canopies and stand growth. Pages 21–39 *in* G. Russell, B. Marshall, and P. G. Jarvis, editors. Plant canopies: their growth, form and function. Cambridge University Press, New York, New York, USA.

Salisbury, F. B., and C. Ross. 1969. Plant physiology. Wadsworth, Belmont, California, USA.

Schimel, D. S. 1995. Terrestrial biogeochemical cycles: global estimates with remote sensing. Remote Sensing of Environment **51**:49–56.

Sellers, P. J. 1987. Canopy reflectance, photosynthesis, and transpiration. II. The role of biophysics in the linearity of their interdependence. International Journal of Remote Sensing **6**:1335–1372.

Sellers, P. J., R. E. Dickinson, D. A. Randall, A. K. Betts, F. G. Hall, J. A. Berry, G. J. Collatz, A. S. Denning, H. A. Mooney, C. A. Nobre, N. Sato, C. B. Field, and A. Henderson-Sellers. 1997. Modeling the exchange of energy, water, and carbon between continents and the atmosphere. Science **275**:502–509.

Shultis, J. K., and R. B. Myneni. 1988. Radiative transfer in vegetation canopies with anisotropic scattering, Journal of Quantitative Spectroscopy and Radiative Transfer **39**: 115–129.

Stoner, E. R., and M. F. Baumgardner. 1981. Characteristic variations in reflectance on surface soils. Soil Science Society of America Journal **45**:1161–1165.

Thomas, J. R., L. M. Namken, G. F. Oerther, and R. G. Brown. 1971. Estimating leaf water content by reflectance measurements. Agronomy Journal **63**:845–847.

Tothill, J. C., and J. J. Mott. 1985. Ecology and management of the world's savannas. Australian Academy of Sciences, Canberra, Australia.

van Leeuwen, W. J. D., and A. R. Huete. 1996. Effects of standing litter on the biophysical interpretation of plant canopies with spectral indices. Remote Sensing of Environment **55**:123–134.

Verdebout, J., S. Jacquemoud, and G. Schmuck. 1994. Optical properties of leaves: modelling and experimental studies. Pages 169–191 *in* J. Hill and J. Megier, editors. Imaging spectrometry—a tool for environmental observations. Kluwer Academic, Dordrecht, The Netherlands.

Walter-Shea, E. A., B. L. Blad, C. J. Hays, M. A. Mesarch, D. W. Deering, and E. M. Middleton. 1992. Biophysical properties affecting vegetative canopy reflectance and absorbed photosynthetically active radiation at the FIFE site. Journal of Geophysical Research **97**:18 925–18 934.

Walter-Shea, E. A., and J. M. Norman. 1991. Leaf optical properties. Pages 229–252 *in* R. B. Myneni and J. Ross, editors. Photon–vegetation interactions, Springer-Verlag, Berlin, Germany.

Wessman, C. A., and G. P. Asner. 1998. Ecosystems and the problems of large-scale measurements. *In* P. Groffman and M. Pace, editors. Successes, limitations, and frontiers in ecosystem ecology. Springer-Verlag, Berlin, Germany, *in press.*

Wooley, J. T. 1971. Reflectance and transmittance of light by leaves. Plant Physiology **47**:656–662.

Young, M. D., and O. T. Solbrig. 1993. The world's savannas: economic driving forces, ecological constraints and policy options for sustainable land use. Parthenon, Carnforth, UK.